The asymmetric rotor as a model for localization

A. R. P. Rau

Department of Physics & Astronomy, Louisiana State University, Baton Rouge, Louisiana 70803

Together with the pendulum, the symmetric and asymmetric rotors are standard models, well studied in both classical and quantum physics. In the limit of high angular momentum J, the quantum problem of an asymmetric rotor approaches the classsical limit, which is characterized by one unstable and two stable motions. Rotations with respect to the axes with maximum and minimum moments of inertia are stable, while the rotations about the intermediate axis are unstable. Upon diagonalization of the rotor's Hamiltonian at fixed J, most eigenvectors are seen to be localized around the directions of maximum and minimum moment of inertia. The asymmetric rotor displays in this regard localization similar to that in many atomic and nuclear few-body systems, wherein external interactions mix degenerate states, particularly at high excitation. Indeed, there is a complete one-to-one correspondence between the rotor and these systems, with the principal (n) and angular momentum (l) quantum numbers mapping onto J, and its azimuthal projection M, respectively, for the rotor. Localization at a maximum or a saddle point of a potential is of considerable significance in a variety of problems.

CONTENTS

I. INTRODUCTION

Much of a physicist's intuition rests on the behavior of a few simple systems. Thus the oscillations of a simple spring or pendulum constitute central elements of the physicist's vocabulary, whether in classical or quantum physics. When we encounter a quadratic interaction in a realm unrelated to a real spring or pendulum, we are apt to exclaim "This is nothing but *the* pendulum," immediately embracing a host of implications. In any listing of such fundamental metaphors of physics, the pendulum (oscillator) and the rotor are two systems that will surely have pride of place.

In multidimensional quantum mechanics, the isotropic oscillator and the symmetric rotor are characterized by degeneracies of their energy levels, particularly large at high excitation. States differing in certain angular momentum quantum numbers share the same energy. Perturbations that destroy the isotropic symmetry lift these degeneracies and lead to large mixings of the degenerate base states of such energy manifolds. A striking consequence of such mixings is the appearance of wave functions that are sharply localized in space, since angles and angular momentum quantum numbers are conjugate variables.

Phenomena characterized by sharp spatial localizations have drawn much interest in diverse areas of physics (Fishman, Grempel, and Prange, 1984; several papers in the collections edited by Taylor, Clark, and Nayfeh, 1988 and Nicolaides, Clark, and Taylor, 1990). This article aims at highlighting the interconnectedness of such diverse phenomena by mapping them onto the fundamental examples of the oscillator and the rotor. Further, these two systems are themselves intimately connected, so that many real physical systems in atomic, nuclear, and many-body physics can be viewed in terms of a single unifying theme, that of a three-dimensional rotor. Degenerate manifolds in these systems can be mapped by one-to-one correspondence to an angular momentum manifold, whereby a wide variety of quadratic interactions that arise in concrete problems map onto the Hamiltonian of an asymmetric rotor.

Crucial common features can thus be understood in terms of the language of the asymmetric rotor where they are more familiar (Townes and Schawlow, 1975; Harter, 1986). Among these are the appearance of localized states, specifically of (two) different classes of such states localized in different spatial regions (or directions), and the attendant implication of negligible overlap between the classes, which leads to long-term stability in spite of the high excitation. This result in the classical limit of high angular momentum can be understood in terms of the discussion of the asymmetric rotor in classical mechanics. Standard texts such as the one by Sommerfeld (1952) show that the rotor displays stability with respect to rotation about two axes, those with the minimum and maximum moments of inertia. The correspondence between atomic and other many-body systems and the rotor then makes plausible that the result carries over to physical systems in the quasiclassical limit at high excitation (large-energy quantum number). Long-term stability in a small local region also has obvious implications for questions of ergodicity and chaos, and for experimental traps for atoms or charged particles [a nice illustration is given in W. Paul's Nobel lecture (Paul, 1990)], so that it is no surprise that the asymmetric rotor also arises in these contexts.

II. THE OSCILLATOR AND ROTOR IN CLASSICAL MECHANICS

A. The one-dimensional oscillator

The beginnings of physics lie in the one-dimensional simple pendulum or harmonic oscillator in classical mechanics. The equations of motion are

$$m\ddot{x} = -(mg/l)x \;, \tag{1a}$$

or

$$\ddot{\theta} = -(g/l)\theta \tag{1b}$$

(with dots representing derivatives with respect to time), and correspond to the potential

$$V(x) = \tfrac{1}{2}kx^2 = \tfrac{1}{2}(mgl)\theta^2 \;, \tag{2}$$

with spring constant $k \equiv m\omega^2 = mg/l$ (Fig. 1). Such a potential traps a one-dimensional mass point at $\theta = x = 0$ with zero energy; at small excitation energies, the mass executes simple harmonic oscillations about that point, with θ a trigonometric function of time with frequency ω.

For negative spring constant k, the potential is an inverted parabola, and the particle is no longer trapped at $x=0$, sliding off instead to arbitrarily large x (exponential, runaway solutions). Stability at the global level can, however, be restored by adding an anharmonicity as in Fig. 2,

$$V(x) = -\tfrac{1}{2}kx^2 + \tfrac{1}{4}\lambda^2 x^4 \;. \tag{3}$$

This double-minimum potential has two symmetrical valleys at $x = \pm k/\lambda$, which can receive the mass point when it rolls off the unstable position at the origin. Such a potential, or its multidimensional generalization, finds wide use in physics: macroscopic quantum tunneling (Leggett *et al.*, 1987), phase transitions as in the Ginzburg-Landau theory (Schrieffer, 1964), inflationary models for the early universe (Weinberg, 1989), the generation of baryon asymmetry (Shaposhnikov, 1987, 1988), field theories of broken symmetry that exhibit the Goldstone phenomenon (Aitchison and Hey, 1989), and the topology of cosmic domains (Kibble, 1976). Even though the potential is symmetric, a classical particle in its ground state will sit asymmetrically at the bottom of one of the wells. With x replaced by a field variable φ, Eq. (3) gives the so-called φ^4 Lagrangian for the scalar field. Rotating the potential in Fig. 2 around the vertical axis produces the so-called "Mexican hat" potential of this scalar field theory. The bottom groove of the hat, which is a circle around the vertical axis at the nonzero value $\varphi = \varphi_0 \equiv k/\lambda$, represents the Goldstone boson, a zero-energy mode of excitation of the field around its minimum "vacuum" value φ_0.

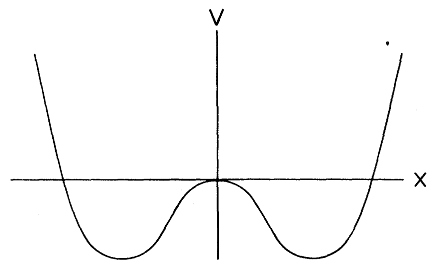

FIG. 2. Double-minimum anharmonic oscillator potential in Eq. (3).

The quartic potential in Eq. (3) is also the first step in the passage from the quadratic potential in Eq. (2) to the full potential of a true pendulum. This potential is indeed nonlinear, as is well known (Goldstein, 1951), so that Eqs. (1b) and (2) are actually linearized versions of

$$\ddot{\theta} = (g/l)\sin\theta \;, \quad V = mgl(1+\cos\theta) \;. \tag{4}$$

We have made a change in the definition of θ to set its zero at the vertically up position, so that this θ differs by π from its value in Eqs. (1) and (2) and Fig. 1. A quartic potential results upon retaining the first two terms in the expansion of $1+\cos\theta$, the full potential being actually given by the solid line in Fig. 3. The equations of motion of the nonlinear pendulum are, of course, more difficult to solve than the freshman-physics problem posed by Eq. (1), requiring the use of elliptic functions rather than the trigonometric ones (Sommerfeld, 1952, Section III.15).

The potential in Eq. (4), as sketched in Fig. 3, already exemplifies a generic feature that will appear as one running theme throughout this article, namely, the existence of stable motions separated by unstable ones. As in Fig. 4(a), the former constitutes the familiar example of a pen-

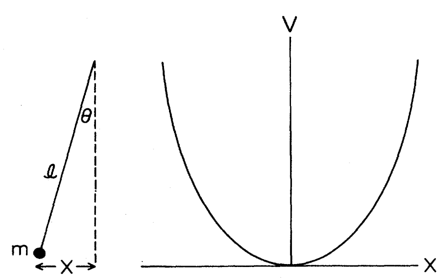

FIG. 1. A simple pendulum and its associated oscillator potential.

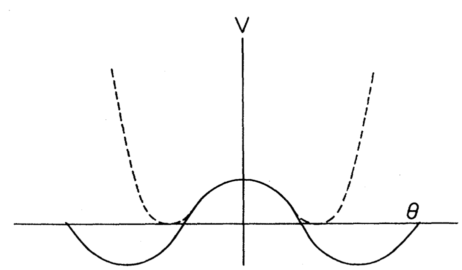

FIG. 3. Potential in Eq. (4): solid curve, for a nonlinear pendulum; dashed curve, for a quartic approximation to it as in Fig. 2.

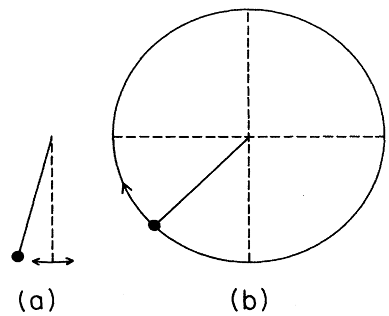

FIG. 4. Two motions of a pendulum: (a) small-amplitude harmonic oscillations; (b) rotation about the point of suspension.

dulum with bob hanging down and making small-amplitude vibrations. The unstable position corresponds to the bob's being vertically up. From that position, the pendulum will fall into one of the valleys on either side at $\theta=\pm\pi$, where, at low energies, it would execute harmonic oscillations. But, at high energies we can also envisage another stable state for the pendulum, namely, full rotation with angular velocity ω in the vertical plane, as shown in Fig. 4(b). Thus, the real (nonlinear) pendulum already exhibits two kinds of states, oscillations and rotations (Goldstein, 1951). Typically, the latter occur only at higher energies. We shall next see that the same result of two classes of states is true also for a rotor. The existence of *two* types of stable motions will be a persistent theme throughout this paper.

Before turning to the rotor, however, it is interesting to note how the rotational motion of the pendulum in Fig. 4(b) in a two-dimensional plane contains within it harmonic oscillatory motion. Projecting the instantaneous position of the bob's rotation onto either the horizontal or the vertical axis yields simple harmonic motion along either axis. This association of harmonic motion along a line with uniform rotation around a circle is used as a formal device already in freshman physics to establish a relationship between oscillations and rotations, but a real pendulum incorporates both types of motions as concrete physical realizations of its dynamics.

B. The rotor

The three-dimensional isotropic rotor has the Hamiltonian

$$H=AJ^2=A(J_x^2+J_y^2+J_z^2)\ , \tag{5}$$

where $\mathbf{J}$ is the angular momentum and $1/(2A)$ the moment of inertia. For fixed angular momentum of rotation, the energy of the isotropic rotor is also a constant, AJ^2. Considering next the symmetric rotor, with one axis having a different moment of inertia,

$$H=A(J_x^2+J_y^2)+CJ_z^2\ ,\quad A>C\ , \tag{6}$$

the energy varies between CJ^2 and AJ^2 as shown in Fig. 5. Note the immediate resemblance to the double-minimum potential of Fig. 2, with $J_z=0$ a maximum and

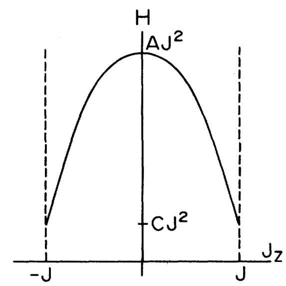

FIG. 5. Hamiltonian of symmetric rotor in Eq. (6) at fixed angular momentum J.

$|J_z|=J$ minima lying on either side. Unlike the x variable in Fig. 2, J_z is constrained to lie in the finite interval $(-J,J)$. Note also, particularly for the later quantum-mechanical discussion in Sec. III, that the dependence on J_z around the maximum is quadratic, while the energy is linear in $J-|J_z|$ in the vicinity of the minimum. These are, respectively, the well-known rotational and librational (vibrational) motions of the torque-free motions of a symmetric rotor.

Apart from an irrelevant overall multiplicative factor, the symmetric rotor in Eq. (6) depends only on one parameter, the so-called "asphericity" $(A-C)$. Spherical symmetry no longer obtains, but cylindrical symmetry is still retained. The fully asymmetric rotor, on the other hand, with Hamiltonian[1]

$$H=AJ_x^2+BJ_y^2+CJ_z^2\ , \tag{7}$$

is characterized by two independent constants, the second being the so-called "asymmetry parameter" (Townes and Schawlow, 1975),

$$\kappa=(2B-A-C)/(A-C)\ . \tag{8}$$

The Hamiltonian in Eq. (7) can be recast in a more transparent form to display the asphericity and asymmetry,

$$H=\tfrac{1}{2}(A+C)J^2+\tfrac{1}{2}(A-C)(J_x^2+\kappa J_y^2-J_z^2)\ . \tag{9}$$

The specifically asymmetric part of the Hamiltonian is contained in the expression in the last parenthesis. This expression is often regarded as the standard form of the asymmetric rotor Hamiltonian. Note that it involves only one constant, κ. It is often customary to label the three axes of inertia so that $A\geq B\geq C$, in which case $-1\leq\kappa\leq 1$.

---

[1]For a rotor, the coordinates (x,y,z) refer to its body frame and are often denoted by primes or by Greek letters in the literature. Likewise, the quantum number for the projection of the rotor's angular momentum onto its body-fixed z axis is usually denoted by K. In this paper, where the focus is entirely on the body frame with no reference to laboratory axes, Cartesian symbols have been used for the coordinates and M for the quantum number. With this language, Eq. (7) and the subsequent discussion can apply equally well to a quadrupolar Hamiltonian, which is isomorphic to that of the asymmetric rotor (Landau and Lifshitz, 1977, Section 103).

Torque-free motion of an asymmetric rotor in space displays libration, rotation, and a so-called separatrix motion. It has long been recognized that rotations with respect to the axes with minimum and maximum moments of inertia are stable, but motion with respect to the intermediate axis results in a tumbling, unstable motion[2] (Sommerfeld, 1952, Section IV.26). Note the reoccurrence of the theme of alternating stable and unstable motions. Sommerfeld discusses these motions of a rotor with reference to tossing a matchbox into the air while simultaneously spinning it. The intermediate or separatrix motion manifests itself in the blurred image seen as different faces of the box present themselves to the eye during its tumbling motion. In our own times, NASA astronauts have demonstrated these motions under the free fall conditions inside the orbiting Space Shuttle.

To see the correspondence between the nonlinear pendulum in Eq. (4) and the asymmetric rotor, let us rewrite Eq. (7) at some fixed total angular momentum J and projection J_z onto the z axis. Setting $J_x=(J^2-J_z^2)^{1/2}\cos\varphi$, $J_y=(J^2-J_z^2)^{1/2}\sin\varphi$, we have

$$H=\tfrac{1}{2}(A+B)J^2+[C-\tfrac{1}{2}(A+B)]J_z^2 + \tfrac{1}{2}(J^2-J_z^2)(B-A)\cos 2\varphi \ . \tag{10}$$

Apart from the first term, which is merely an additive constant to the energy, the other two terms in Eq. (10) are as in Eq. (4) except in a more general form, involving two constants rather than the single constant mgl. Both problems share the same general features in the structure of their Hamiltonians and of its solutions. Both display librations, typically at low energy, and rotations, usually at higher energies, with a separatrix marking the transition between these two kinds of motion. Diverse problems in nonlinear dynamics share these same characteristics and, therefore, the nonlinear pendulum has served as a universal model for them. This is the so-called "Chirikov paradigm" (Chirikov, 1979; see also Aquilanti, Cavalli, and Grossi, 1984, 1985), which regards forced oscillation of the nonlinear pendulum in Eq. (4) as a general illustration of stochasticity. When such a pendulum is driven by an external force with frequency Ω that is close to $\omega=(g/l)^{1/2}$, the frequency of the nonlinear oscillations varies in a manner unlike a linear resonance, because the amplitude varies. Both amplitude and frequency display, therefore, beat frequencies $\Delta\omega$. If the driving force has a distribution of frequencies $\Delta\Omega$ that is less than $\Delta\omega$, then the pendulum oscillates as if under a random force (Zaslavskii and Chirikov, 1972). Such stochastic behavior is seen in many nonlinear problems, including practical ones such as the nonlinear oscillation of charged particles in accelerators and plasmas. Because of its slightly more general form, the asymmetric rotor has been advocated more recently as a more general and suitable candidate for the Chirikov mapping (Sahm, McWhorter, and Uzer, 1989).

The asymmetric rotor and the pendulum are, therefore, essentially equivalent physical systems. The solutions of the equations of motion involve elliptic functions in both cases. Both systems display oscillatory and rotational motions. From now on, we shall focus on the asymmetric rotor and demonstrate its usefulness as a model for many microscopic quantum systems that also exhibit vibrational and rotational states.

III. LOCALIZATION PHENOMENA IN QUANTUM SYSTEMS

A. Highly excited atom in a magnetic field

As an illustrative example of diverse systems in microscopic quantum mechanics whose study in recent years has pointed to certain common, dominant features, consider an atom in a magnetic field **B**. For a given magnetic field, there is always a principal quantum number n above which the interaction with the field is no longer perturbative. At such high excitations of a single electron, the role of the remaining atomic electrons is not an essential feature; it thus suffices to consider the simplest atom, hydrogen. The linear Zeeman term in the coupling to the magnetic field gives only an additive contribution to the energy, depending on the value of the m quantum number of the electron. This quantum number, along with parity, remain good quantum numbers, and we can restrict ourselves to one value of m^{π}. The quadratic, diamagnetic interaction with the magnetic field breaks, however, the spherical symmetry of the hydrogen Hamiltonian, leaving only a residual cylindrical symmetry. The combined Coulomb and diamagnetic interaction gives the potential

$$V(r,\theta)=-(e^2/r)+(e^2/8mc^2)B^2r^2\sin^2\theta \ . \tag{11}$$

Remarkably, this nonrelativistic Hamiltonian describing the seemingly simple situation of a hydrogen atom in a constant, static magnetic field (along the z axis) has provided surprises unanticipated through the first-fifty-year history of atomic physics. In spite of its simplicity, the Schrödinger equation with this potential cannot be solved exactly. Nevertheless, recent experiments on this system have uncovered qualitatively new and unexpected structures in the spectrum (Nicolaides, Clark, and Nayfeh, 1990). Figure 6 provides an illustration. This is a high-

---

[2]For an asymmetric rotor, spinning about one of its principal axes (say C), with angular momentum $\mathbf{J}$ and energy $E=CJ^2$, departures of the angular frequency $\boldsymbol{\omega}$ from its value $\boldsymbol{\omega}_0=2C\mathbf{J}, \boldsymbol{\omega}=\boldsymbol{\omega}_0+\boldsymbol{\varepsilon}$ obey the relation (Hestenes, 1986, p. 489)

$$(C-A)(\varepsilon_A/A)^2+(C-B)(\varepsilon_B/B)^2=4(CJ^2-E) \ .$$

This is the equation of an ellipse and $\boldsymbol{\omega}$ will, therefore, stay in the vicinity of $\boldsymbol{\omega}_0$ if C is either larger or smaller than both A and B. If C is the intermediate axis, on the other hand, the above equation describes a hyperbolic departure of $\boldsymbol{\varepsilon}$ away from zero, so that the motion is unstable.

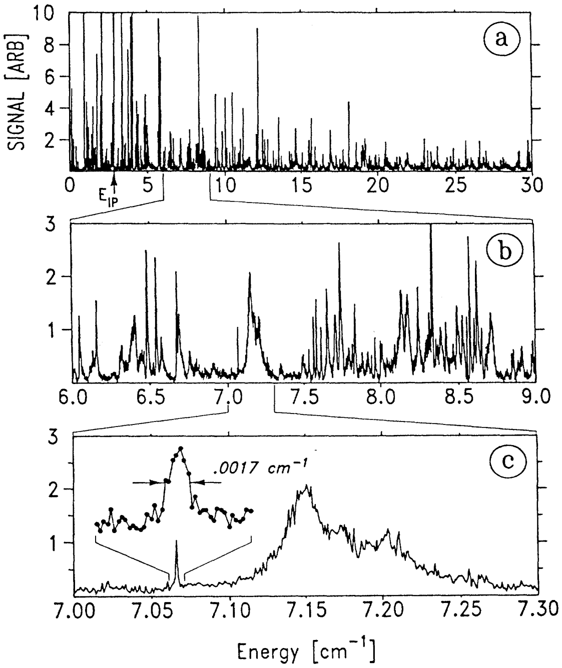

FIG. 6. High-resolution photoabsorption spectrum of lithium above the zero-field ionization limit in a magnetic field of 6.1 T. Note the wealth of sharp lines, 1 $\mathrm{cm}^{-1} \simeq 0.124$ meV $\simeq 30$ GHz (from Welch *et al.*, 1989).

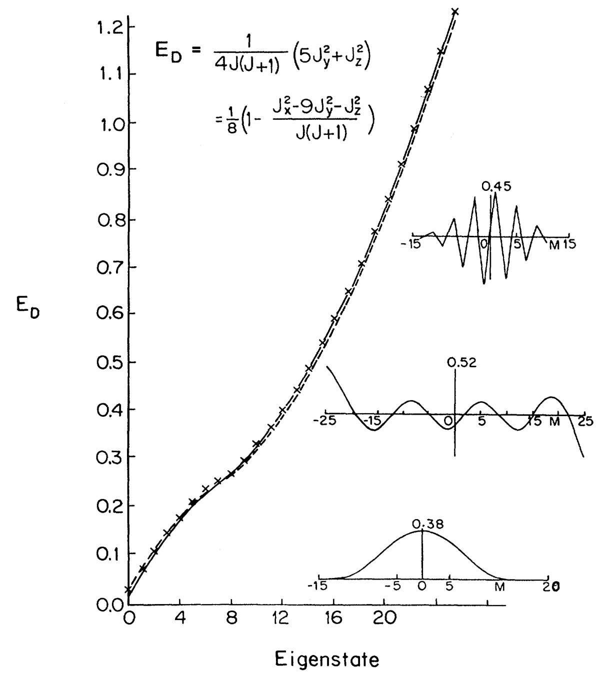

FIG. 7. Diamagnetic interaction in a hydrogenic manifold as an asymmetric rotor: x, eigenvalues of the scaled, dimensionless diamagnetic potential $\frac{1}{2}r^2\sin^2\theta/(n^4a_0^2)$ in Eq. (11), where a_0 is the Bohr radius, for $n=51$; solid curve, eigenvalues of the asymmetric rotor for $J=50.5$; dashed curve, eigenvalues of the asymmetric rotor for $J=25$ and asymmetry parameter $\kappa=-9$. Note two types of eigenvalue spacings, separated by a separatrix at 0.25. Also shown alongside are the highest, the separatrix, and the lowest eigenvectors for $J=25$, along with their peak amplitudes (from Rau and Zhang, 1990).

resolution spectrum in the vicinity of the zero-field ionization limit of the atom (Welch *et al.*, 1989; Iu *et al.*, 1991). There is a wealth of sharp structures even at positive energies (which is the region of a smooth featureless continuum when $B=0$), one feature having been singled out with a width less than 0.0017 cm^{-1}. This is a pointer to extremely long-lived, almost stable spectral levels in a region of very high excitation, where either field alone supports only continuum states. In the partial theoretical understanding that has been gained of such quasistable features and of other phenomena associated with Eq. (11), the existence of states very localized in θ plays an essential role. A variety of studies (Taylor, Clark, and Nayfeh, 1988; Rau, 1989; Nicolaides, Clark, and Nayfeh, 1990; Rau and Zhang, 1990) of Eq. (11) have pointed to two classes of localized states, one concentrated longitudinally along the field ($\theta=0,\pi$) and another perpendicular to the field ($\theta=\pi/2$). The latter, in particular, are responsible for the sharp spectral features, because an electron trapped in a motion transverse to the field cannot escape, escape to infinity being possible only along the field lines.

The breaking of spherical symmetry and the lifting of the l degeneracy of atomic energy levels lead to strong mixing of the different $|nl\rangle$ states at any fixed n. Indeed, studies (Braun, 1983a, 1983b; Fano, Robicheaux, and Rau, 1988) show that diagonalization of the interaction in Eq. (11) gives a spectrum like that in Fig. 7. At the lower energy end, the levels are equally spaced as in an oscillator, but develop the pattern of a rotor above a certain critical "separatrix" (Herrick, 1981; Soloviev, 1981; Gay *et al.*, 1983) value ($\frac{1}{4}$ in the figure). Examination of the eigenvectors by translating the superposition in l to the corresponding distribution in θ shows that the lowest eigenstates are localized longitudinally and the highest ones transversely to the magnetic field; the localization becomes sharper with increasing excitation, that is, increasing n. These results are immediately reminiscent of the earlier discussion of the asymmetric rotor. Indeed, the quantum treatment of this Hamiltonian in Eq. (7) at fixed J^2 gives the same kind of eigenvalue and eigenvector structure as for an atom in a magnetic field, as also shown in Fig. 7 (Braun, 1983a; Rau and Zhang, 1990; Uzer, 1990).

Yet, superficially, the Hamiltonian in Eq. (11) does not suggest immediately any such link to the asymmetric rotor Hamiltonian in Eq. (7). The link rests on the following. The degenerate manifold of hydrogenic states $|nl\rangle$ with $l=0,1,\ldots(n-1)$ is analogous to an angular momentum manifold $|JM\rangle$, $M=-J, -J+1,\ldots,J-1, J$. The diamagnetic interaction in Eq. (11) is tridiagonal in the former manifold ($\sin^2\theta$ has nonzero matrix elements only between l and $l'=l\pm2$), just as the quadratic asymmetric rotor Hamiltonian in Eq. (7) is tridiagonal in the $|JM\rangle$ basis with $M\to M, M\pm2$. In the $|JM\rangle$ basis,[1]

J_z^2 in Eq. (7) is diagonal and the other two terms in J_x^2 or J_y^2 are bilinear products of the step operators, $J_\pm = J_x \pm iJ_y$, in the angular momentum manifold. Since the manifold terminates at $M = \pm J$, the matrix elements of these operators have factors involving $(J \mp M)$, and the off-diagonal matrix elements of Eq. (7) are therefore proportional to $[1 - M^2/(J+\frac{1}{2})^2]$. Turning to Eq. (11) and its action on $|nl\rangle$ states, we have an exactly analogous situation. Examination of off-diagonal matrix elements of r^2 (or, for that matter, other powers of r) between radial hydrogenic functions shows that they vanish when $l \to n$, the edge of the manifold. In fact, such matrix elements involve the factors $(n-l)\,(n+l+1)$, analogous to the $(J \pm M)\,(J \mp M+1)$ factors in the action of $J_\mp$. These comparisons, together with the standard semiclassical replacement of l by $l+\frac{1}{2}$, suggest that the off-diagonal radial matrix elements vanish in two limits $l+\frac{1}{2} \to \pm(n-\frac{1}{2})$ so that, both in the structure of the manifold and in the matrix elements within the manifold, there is an exact correspondence $J \to (n-\frac{1}{2})$, $M \to (l+\frac{1}{2})$ (Rau and Zhang, 1990).

B. General tridiagonal interactions

The correspondence in the previous paragraph is one of great generality. Many interactions, besides the diamagnetic one in Eq. (11), which are quadratic in the sense that they are tridiagonal in the degenerate basis $|nl\rangle$, map one-to-one onto the problem of the asymmetric rotor, whose Hamiltonian is the most general quadratic interaction in a $\{|JM\rangle\}$ manifold. It also follows, without any detailed consideration of the specific interaction, that this tridiagonal matrix has a generic form specified by three constants: In terms of the variable $u = (l+\frac{1}{2})/n$, the diagonal matrix elements are $v_0 - v_1 u^2$ while the off-diagonal matrix elements, which vanish as $u \to 1$, are $w(1-u^2)$, with three constants v_0, v_1, and w. These constants take the place of A, B, and C of the rotor and, indeed, we can read off from Eq. (10)

$$\begin{aligned} v_0 &= \tfrac{1}{2}(A+B)\,, \\ v_1 &= \tfrac{1}{2}(A+B) - C\,, \\ w &= \tfrac{1}{4}(A-B)\,. \end{aligned} \tag{12}$$

This mapping of diverse problems onto an asymmetric rotor has been demonstrated (Rau and Zhang, 1990) for several problems in atomic physics where other interactions—for instance, with an electric field—replace the second term in Eq. (11), and also in nuclear physics, where again one has a degenerate $\{|nl\rangle\}$ manifold of the shell-model potential $\frac{1}{2}r^2$ as the starting basis. A canonical interaction in nuclear models is the quadrupole, $r^2 Y_2^0$, which, of course, is of exactly the same form as the asymmetric rotor Hamiltonian in Eq. (7). The algebraic diagonalization of all these tridiagonal problems can be converted (Fano, Robicheaux, and Rau, 1988; Rau, 1989) to second-order differential equations for spheroidal functions or, equivalently, Mathieu functions (Abramowitz and Stegun, 1965). These are also closely related to the Lame functions that were used in the classic study of the asymmetric rotor by Kramers and Ittmann (1929, 1930). Note that in the quantum treatment of Eq. (4) or (10), the Hamiltonian has the form of a constant plus a term in the cosine of the variable, as in the Sturm-Liouville equation for Mathieu functions. The Mathieu functions are the quantum counterpart of the elliptic functions arising in the classical mechanical treatment of these problems. Braun (1978, 1983a, 1983b, 1989) has used a so-called discrete WKB method to study the diamagnetic and other tridiagonal problems and has also related them to the asymmetric rotor.

Eigenvalues of these tridiagonal matrices lie between $v_0 - 2w$ and $v_0 + 2w$, with the separatrix at $v_0 - v_1$. The eigenvalues are equally spaced at either end of the spectrum. The eigenvectors at the ends involve superpositions of many l values (up to a maximum of approximately $n^{1/2}$) in a form that yields a sharp localization in the conjugate angle θ. Only for a few states near the separatrix are the eigenvectors roughly uniformly spread over all l (Fano, Robicheaux, and Rau, 1988). In the language of the asymmetric rotor, the two classes of states at the ends involve superpositions of M with $|M| \le J^{1/2}$ and correspond to rotations about the minimum and maximum moments of inertia, while the states near the separatrix, which include also the high $|M|$ values (see Fig. 7), correspond to rotations about the intermediate axis. The well-known classical result for the rotor, that the former two motions are stable while the intermediate one is unstable, accounts for the fact that at large n most states are localized in two different regions of coordinate space, only a few in separatrix region. These separatrix states represent, however, the connection between the states localized in different regions. [In the initial example of the pendulum in Fig. 4, the separatrix, which makes the boundary between oscillations and rotations, lies at the unstable "up" position (Chirikov, 1979, Section 2-4).] All these considerations are obviously very relevant both to long-term stability (trapping) in confined regions and to questions of chaos when the system can be thrown from one region to another (Aquilanti, Cavalli, and Grossi, 1985; Casati, 1985).

The central result that most of the states in these tridiagonal problems are localized (either longitudinally or transversely, for a highly excited atom in a magnetic field) hinges on the vanishing of the off-diagonal coupling $w(1-u^2)$ at the edges of the spectrum, $u \to \pm 1$. In turn, as developed in the last paragraph of Sec. III.A, this results from the vanishing of couplings involving ladder operators within a degenerate manifold as $l \to n$ or $|M| \to J$. This result contrasts with a tridiagonal problem lacking this feature, such as the one-dimensional Kronig-Penney model with constant nearest-neighbor coupling (Kittel, 1956). In this case, nearly all states extend throughout the one-dimensional lattice, with only a few localized in "band gaps." These contrasting results are, of course, conjugates, constant coupling in a spatial coordinate being equivalent to sharply localized interaction in the corresponding momentum space. Note also the contrast between the localization we have discussed above and the one in disordered systems (Fishman, Grempel, and Prange, 1984). While both deal with tridiagonal matrices, we have associated localization with the vanishing of the off-diagonal coupling towards the edges, whereas the so-called "Anderson localization" arises from the random nature of the diagonal matrix elements.

IV. STABILITY AT SADDLE POINTS

In the atomic diamagnetic problem, two groups of states are localized around $\theta=0$, the minimum of the potential in Eq. (11), and around $\theta=\pi/2$; the latter are more intriguing because they lie at a maximum of the potential and are responsible for new and surprising phenomena (Nicolaides, Clark, and Nayfeh, 1990). In the asymmetric rotor, once again the stability of rotations with respect to the axis with minimum moment of inertia (therefore, maximum energy) is rather surprising.[2] We further illustrate this stability, and the essential role of coupling between motions in different directions, through the model of a two-dimensional oscillator with one spring constant negative,

$$V(x,y)=\tfrac{1}{2}k_1x^2-\tfrac{1}{2}k_2y^2 \ . \tag{13}$$

Figure 8 shows a sketch of this potential, whose origin lies at a saddle point. In a multidimensional space, most extrema are likely to be saddle points, the potential falling off in certain directions and rising in others for departures from that point. The study of the behavior near saddle points is thus necessary to understand dynamics in many dimensions. Clearly, a mass m placed at the origin will not be stable because it can run downhill in the y direction following the slightest perturbation.

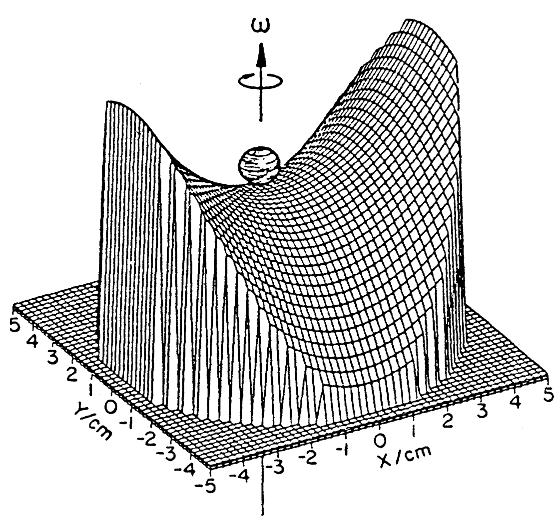

FIG. 8. Mechanical model of a saddle potential surface. A mass point can be held at the saddle if the turntable on which the saddle stands is rotated around the vertical axis (from Paul, 1990).

To restore stability, a coupling has to be provided between the x and y motions, as in the following mechanical model. If the potential surface in Fig. 8 is mounted on a turntable and set into sufficiently rapid rotation, then indeed a particle can be trapped in the vicinity of the origin. In fact, this example and the figure are drawn from W. Paul's Nobel Lecture (Paul, 1990), where they are used as analogs of the electromagnetic trap devised by him for charged particles. It is well known that a purely electrostatic field cannot trap a charged particle in all directions simultaneously. [Thus, for instance, a (quadrupole) potential such as $V=x^2+y^2-2z^2$ must have one of its terms negative to satisfy $\nabla^2V=0$.] Adding an oscillating field and thereby introducing a time element and a link between different directions, Paul was able to devise a trap for charged particles. Thus, for instance, in the mechanical example in Eq. (13) and Fig. 8, if x and y are parametrically linked (through rotation of the turntable) as trigonometric functions of time, the equations of motion become once again Mathieu functions (Paul, 1990), and the problem maps onto an asymmetric rotor (Rau and Zhang, 1990). Time-varying quadrupole fields which induce oscillations of the charged particles, also described by the Mathieu equation, also play a critical role in the focusing of such beams in high-energy accelerators (Humphries, 1986). For another interesting mechanical example of an added time element's restoring stability, consider again the pendulum. The vertically up position is unstable, but if the base is jiggled up and down with a frequency Ω, the pendulum is stable for bands of values of Ω. The equation of motion is again that of Mathieu functions (Jaeger and Starfield, 1974).

The above example of stabilization in Fig. 8 through an added rotation is closely similar to the historical problem of stability at "Lagrange points" in the restricted three-body problem in celestial mechanics. Of the five such points (Fig. 9), L_4 and L_5 are maxima of the potential but, nevertheless, can be stable positions for the third body under certain conditions. The Trojan asteroids provide an example in the Sun-Jupiter system. Stability is achieved through the Coriolis force that acts to deflect the particle when it runs down from the peak, causing it to climb back uphill (Hestenes, 1986, p. 411).

A coupling between the x and y motions may also be

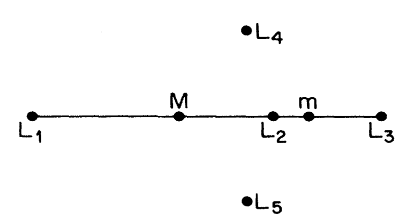

FIG. 9. Extrema of the gravitational potential, called Lagrange points, for two bodies of mass M and m.

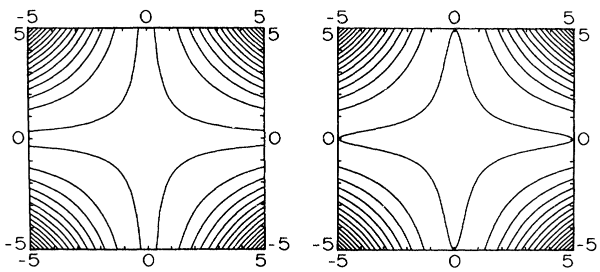

FIG. 10. Potential-energy contours for the quartic two-dimensional potential in Eq. (15) for $\beta=0$ (left) and $\beta=0.01$ (right). Note valleys along the axes and ridges along the diagonals (from Zakrzewski and Marcinek, 1990).

introduced without resorting to time dependence, fitting in more naturally with the rest of this paper. Consider, for instance, the two-dimensional potential (Pullen and Edmonds, 1981)

$$V(x,y)=\tfrac{1}{2}(x^2+y^2)+\alpha x^2y^2 , \tag{14}$$

which has been much studied in the literature on chaos, or the similar quartic potential (Fig. 10)

$$V(x,y)=\tfrac{1}{2}(x^4+y^4)+\beta x^2y^2 . \tag{15}$$

These arise also in Yang-Mills field theories with the group SU(2) (Jackiw and Rossi, 1980; Chang, 1984) and have been discussed in this context in terms of the symmetric rotor and of "vibrational" and "rotational" energies of the gluon field (Savvidy, 1985). Mapping these potentials onto the tridiagonal asymmetric rotor yields one class of localized states along the axes while another one represents "ring" states, as shown in Fig. 11 (Eckhardt, Hose, and Pollak, 1989; Zakrzewski and Marcinek, 1990). The separatrix lies here along the diagonals $x=\pm y$, which mark ridges of the potential surface.

Another quantum-mechanical problem that involves localization at a saddle of a two-dimensional nonseparable potential concerns highly excited states of two-electron atoms near their double ionization limit (Fano and Rau, 1986). In examining the radial aspects of this system, we find that the potential exhibits a maximum when the variable r_1/r_2 is unity. That is, the system is unstable with respect to departures of r_1 and r_2 from equality. If one of the electrons is closer to the nucleus than the other, it screens more of the nuclear field for the other, thereby making the discrepancy in their radial distances even larger. Thus one would at first glance expect no stable states around $r_1/r_2=1$, and classical computation of trajectories would seem to diverge away from this point. However, both numerical computations and other quantum-mechanical analyses show trajectories *converging* to this point and states localized in its vicinity (Fano and Rau, 1986; Rau, 1990). The converging trajectories, which climb uphill in the potential, are analogs of the earlier discussion regarding Lagrange points in celestial mechanics. In that case, the Coriolis force was responsible; likewise, in the two-electron problem, it is the interplay between kinetic and potential terms in the Hamiltonian that leads to the converging behavior. The effect arises from the nonseparable coupling in the full three-body problem between the variable r_1/r_2 and another variable, $R=(r_1^2+r_2^2)^{1/2}$. Trajectories converge and others diverge from $r_1/r_2=1$ as R increases. It is important to consider both sets in accounting for high excitation in the two-electron system. This problem has also been analyzed by mapping onto the asymmetric rotor (Rau and Zhang, 1990).

Localization at a saddle, or a ridge, or a maximum of a potential surface, and the associated quasistable states, play an important dynamical role in wide areas of physics. Ever since the classic work of Eyring and co-workers (Glasstone, Laidler, and Eyring, 1941), the so-called "activated" or "transition" state has been discussed extensively in quantum chemistry as a key mediator in chemical reactions. This transition state resides at a saddle in the potential-energy surface as a function of reaction coordinates and serves as the intermediary in the transformation of the system from one valley to another of the potential surface (Pechukas, 1981; Tachibana, 1982; Truhlar, Isaacson, and Garrett, 1985). Pollak (1983) has even discussed so-called "adiabatic molecules" in light-atom-transfer reactions such as $HI+I \rightarrow I+HI$, wherein the light atom H can be localized at an intermediate saddle point between the two iodine atoms to form the complex IHI, much as in the elementary molecule H_2^+, where the electron similarly resides between the two protons.

Fano (1981, 1983) has held up the two topics discussed earlier in this essay, localization transverse to the magnetic field in highly excited states of atoms and localiza-

FIG. 11. Two types of localized states, "channel" and "ring" types, in the potential shown in Fig. 10 with $\beta=0.01$ for two nearby scaled energies (from Zakrzewski and Marcinek, 1990, adapted from Eckhardt, Hose, and Pollak, 1989).

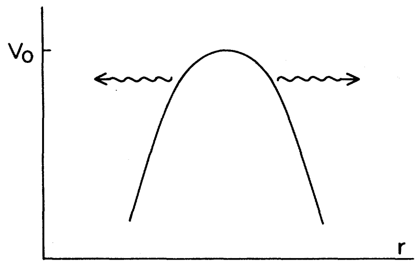

FIG. 12. Purely outgoing waves from a potential barrier, representing barrier-top resonances in nuclear reactions and quasinormal modes of a black hole.

tion at a saddle for highly excited two-electron states, as prototypes of general chemical transformation, and he has emphasized the crucial role of ridge localization in such transformation (see also Aquilanti, Cavalli, and Grossi, 1984). Friedman and Goebel (1977) discussed so-called "barrier-top resonances" in nuclear reactions, particularly between two heavy ions when strong absorption is involved. The combination of Coulomb and centrifugal forces leads to a barrier in the radial coordinate, schematized as an inverted harmonic oscillator in Fig. 12. With the frequency ω replaced by the imaginary $(-i\nu)$, the usual Gaussians in oscillator bound state functions, $\exp(-m\omega x^2/2)$, are replaced by purely outgoing waves, $\exp(im\nu x^2/2)$, away from the barrier. The corresponding states describe resonances with energy $E_n = V_0 - i(n+\frac{1}{2})\nu$. It is the strong absorption at small r, that is, to the left of the barrier in Fig. 12, that permits the existence of such purely outgoing-wave solutions, eliminating the ingoing (reflected) waves from the left which would otherwise be present. Elsewhere, the so-called quasinormal modes of a black hole are similarly described. Once again, the absorptive nature of the "horizon" to the left of the barrier leads to such solutions, which describe the last stages of decay of a perturbed black hole, the observed frequencies being characteristic of the black hole alone and independent of the original cause. Chandrasekhar (1983) refers to them as the "pure dying tones of a perturbed black hole."

V. SUMMARY

The asymmetric rotor serves to study the localization in space of the motion of varied physical systems. Both in their physics and in their mathematics (elliptic functions in classical mechanics, Mathieu functions in quantum mechanics), these systems are unified under the single banner of the asymmetric rotor. In the classical limit of high angular momentum J, we have the classical result that the motions about the two extreme moments of inertia are stable, while rotation about the axis with intermediate moment of inertia is unstable. The corresponding quantum-mechanical result is that the spectrum obtained upon diagonalization of the Hamiltonian in a $|JM\rangle$ basis exhibits equally spaced oscillator-like levels at both ends of the span of eigenvalues, with a separatrix region in between. (In a few special cases the eigenvalues show a symmetric rotor pattern.) Examination of the eigenvectors shows a superposition of M values such that the two groups at either end have localized wave functions in space.

In classical mechanics, the rotor and the nonlinear pendulum are intimately linked and form the basis for many studies of nonlinear dynamics. The existence of different modes, of mode coupling leading sometimes to chaotic evolution, etc., are some of the topics at the heart of the current ferment in the study of chaos (Casati, 1985). In many atomic and nuclear quantum systems, degenerate states $\{|nl\rangle\}$ are mixed by coupling to external fields or to other particles, and the asymmetric rotor is again relevant. The degenerate manifold behaves much like an angular momentum manifold and the interactions within it like the action of the asymmetric rotor Hamiltonian in the $\{|JM\rangle\}$ manifold. In the semiclassical limit of large n these systems also exhibit, therefore, localization that can be described in the language of the asymmetric rotor.

In fact, the mapping onto the rotor is likely to be of even greater generality, applicable to any degenerate manifold, whether or not it is easily identifiable, as in the examples of the $|nl\rangle$ states of a Coulomb or a shell-model Hamiltonian. The existence of a degenerate manifold implies also step operators that can link different states of the manifold. The Lenz vector serves this purpose in the Coulomb problem (Landau and Lifshitz, 1977, Section 36). It has been noted (Aharanov *et al.*, 1990) that there always exists a vector potential in a degenerate manifold of a nonseparable potential, and this vector potential is like the Lenz vector in having off-diagonal matrix elements inside that manifold. Modeling the manifold in terms of $\{|JM\rangle\}$ and of the step operators $J_\pm$ translates the problem into the language of angular momentum. Since the asymmetric rotor has the most general quadratic Hamiltonian in angular momentum space, various quadratic interactions in a general degenerate manifold can be thus translated, accounting for the importance of this system across wide areas of physics.

ACKNOWLEDGMENTS

This essay has benefited greatly from numerous criticisms and suggestions by Dr. U. Fano and Dr. M. Inokuti. This work has been supported by the National Science Foundation.

REFERENCES

Abramowitz, M., and I. A. Stegun, 1965, *Handbook of Mathematical Functions* (Dover, New York), Chaps. 20 and 21.

Aharanov, Y., E. Ben-Reuven, S. Popescu, and D. Rohrlich, 1990, Phys. Rev. Lett. **65**, 3065.

Aitchison, I. J. R., and A. J. G. Hey, 1989, *Gauge Theories in Particle Physics* (Adam Hilger, Bristol), Sec. 13.3.

Aquilanti, V., S. Cavalli, and G. Grossi, 1984, Chem. Phys. Lett. **110**, 43.

Aquilanti, V., S. Cavalli, and G. Grossi, 1985, in *Chaotic Behavior in Quantum Systems: Theory and Applications,* edited by G. Casati (Plenum, New York), p. 299.

Braun, P. A., 1978, Teor. Mat. Fiz. **37**, 355 [Theor. Math. Phys. **37**, 1070 (1978)].

Braun, P. A., 1983a, Zh. Eksp. Teor. Fiz. **84**, 850 [Sov. Phys.—JETP **57**, 492 (1983)].

Braun, P. A., 1983b, J. Phys. B **16**, 4323.

Braun, P. A., 1989, Opt. Spektrosk. **66**, 57 [Opt. Spectrosc. **66**, 32 (1989)].

Casati, G., 1985, Ed., *Chaotic Behavior in Quantum Systems: Theory and Applications,* NATO ASI Series B, Vol. 120 (Plenum, New York).

Chandrasekhar, S., 1983, *The Mathematical Theory of Black Holes* (Oxford University, Oxford), Chap. 4, Sec. 35.

Chirkov, B. V., 1979, Phys. Rep. **52**, 263.

Chang, S. J., 1984, Phys. Rev. D **29**, 259.

Eckhardt, B., G. Hose, and E. Pollak, 1989, Phys. Rev. A **39**, 3776.

Fano, U., 1981, Phys. Rev. A **24**, 2402.

Fano, U., 1983, in *Atomic Physics 8,* edited by I. Lindgren, A. Rosen, and S. Svanberg (Plenum, New York), p. 5.

Fano, U., and A. R. P. Rau, 1986, *Atomic Collisions and Spectra* (Academic, New York), Sec. 10.6.

Fano, U., F. Robicheaux, and A. R. P. Rau, 1988, Phys. Rev. A **37**, 3655.

Fishman, S., D. R. Grempel, and R. E. Prange, 1984, Phys. Rev. A **29**, 1639.

Friedman, W. A., and C. J. Goebel, 1977, Ann. Phys. (N.Y.) **104**, 145.

Gay, J. C., D. Delande, F. Biraben, and F. Penent, 1983, J. Phys. B **16**, L693.

Glasstone, S., K. J. Laidler, and H. Eyring, 1941, *The Theory of Rate Processes* (McGraw-Hill, New York), Chap. 3.

Goldstein, H., 1951, *Classical Mechanics* (Addison-Wesley, Reading), Sec. 9.5.

Harter, W. G., 1986, J. Chem. Phys. **85**, 5560.

Herrick, D. R., 1981, Phys. Rev. A **26**, 323.

Hestenes, D., 1986, *New Foundations for Classical Mechanics* (Reidel, Dordrecht).

Humphries, S., Jr., 1986, *Principles of Charged Particle Acceleration* (Wiley, New York), Sec. 14.6.

Iu, Chun-ho, G. R. Welch, M. M. Kash, D. Kleppner, D. Delande, and J. C. Gay, 1991, Phys. Rev. Lett. **66**, 145.

Jackiw, R., and P. Rossi, 1980, Phys. Rev. D **21**, 426.

Jaeger, J. C., and A. M. Starfield, 1974, *An Introduction to Applied Mathematics* (Clarendon, Oxford), Sec. 104.

Kibble, T. W. B., 1976, J. Phys. A **9**, 1387.

Kittel, C., 1956, *Introduction to Solid State Physics* (Wiley, New York), Chap. 11.

Kramers, H. A., and J. P. Ittmann, 1929, Z. Phys. **53**, 553 (Part I) and **58**, 217 (Part II).

Kramers, H. A., and J. P. Ittmann, 1930, Z. Phys. **60**, 663.

Landau, L. D., and E. M. Lifshitz, 1977, *Quantum Mechanics: Non-Relativistic Theory* (Pergamon, Oxford).

Leggett, A. J., S. Chakravarty, A. T. Dorsey, M. P. A. Fisher, A. Garg, and W. Zwerger, 1987, Rev. Mod. Phys. **59**, 1.

Nicolaides, C. A., C. W. Clark, and M. H. Nayfeh, Eds., 1990, *Atoms in Strong Fields,* NATO ASI Series B, Vol. 212 (Plenum, New York).

Paul, W., 1990, Rev. Mod. Phys. **62**, 531.

Pechukas, P., 1981, Annu. Rev. Phys. Chem. **32**, 159.

Pollak, E., 1983, J. Chem. Phys. **78**, 1228.

Pullen, R. A., and A. R. Edmonds, 1981, J. Phys. A **14**, L477.

Rau, A. R. P., 1989, Phys. Rev. Lett. **63**, 244.

Rau, A. R. P., 1990, Rep. Prog. Phys. **53**, 181.

Rau, A. R. P., and L. Zhang, 1990, Phys. Rev. A **42**, 6342.

Sahm, D. K., S. W. McWhorter, and T. Uzer, 1989, J. Chem. Phys. **91**, 219.

Savvidy, G. K., 1985, Phys. Lett. B **159**, 325.

Schrieffer, J. R., 1964, *Theory of Superconductivity,* Frontiers in Physics No. 20 (Benjamin-Cummings, Reading), p. 19.

Shaposhnikov, M. E., 1987, Nucl. Phys. B **297**, 757.

Shaposhnikov, M. E., 1988, Nucl. Phys. B **299**, 797.

Soloviev, E. A., 1981, Pis'ma Zh. Eksp. Teor. Fiz. **34**, 278 [JETP Lett. **34**, 265 (1981)].

Sommerfeld, A., 1952, *Mechanics* (Academic, New York).

Tachibana, A., 1982, Int. J. Quantum Chem. **22**, 191.

Taylor, K. T., C. W. Clark, and M. H. Nayfeh, 1988, Eds., *Atomic Spectra and Collisions in External Fields* (Plenum, New York).

Townes, C. H., and A. L. Schawlow, 1975, *Microwave Spectroscopy* (Dover, New York), Chap. 4.

Truhlar, D. G., A. D. Isaacson, and B. C. Garrett, 1985, in *Theory of Chemical Reaction Dynamics,* Vol. 4, edited by M. Baer (CRC Press, Boca Raton), p. 65.

Uzer, T., 1990, Phys. Rev. A **42**, 5787.

Weinberg, S., 1989, Rev. Mod. Phys. **61**, 1.

Welch, G. R., M. M. Kash, Chun-ho Iu, L. Hsu, and D. Kleppner, 1989, Phys. Rev. Lett. **62**, 1975.

Zakrzewski, J., and R. Marcinek, 1990, Phys. Rev. A **42**, 7172.

Zaslavskii, G. M., and B. V. Chirikov, 1972, Usp. Fiz. Nauk. **14**, 3 [Sov. Phys. Usp. **14**, 549 (1972)].